

The infrared spectrum of the $\text{H}_2\text{-HCO}^+$ complex

E. J. Bieske, S. A. Nizkorodov, F. R. Bennett, and J. P. Maier

Institut für Physikalische Chemie, Universität Basel, Klingelbergstr. 80, CH-4056, Switzerland

(Received 9 December 1994; accepted 21 December 1994)

A combined experimental and theoretical study of the structural properties of the $\text{H}_2\text{-HCO}^+$ ion-neutral complex has been undertaken. Infrared vibrational predissociation spectra of mass selected $\text{H}_2\text{-HCO}^+$ complexes in the $2500\text{--}4200\text{ cm}^{-1}$ range display several vibrational bands, the most intense arising from excitation of the C–H and H_2 stretch vibrations. The latter exhibits resolved rotational structure, being composed of $\Sigma\text{--}\Sigma$ and $\Pi\text{--}\Pi$ subbands as expected for a parallel transition of complex with a T-shaped minimum energy geometry. The determined ground state molecular constants are in good agreement with ones obtained by *ab initio* calculations conducted at the QCISD(T)/6–311G(2df,2pd) level. The complex is composed of largely undistorted H_2 and HCO^+ subunits, has a T-shaped minimum energy geometry with an $\text{H}_2\cdots\text{HCO}^+$ intermolecular bondlength of approximately 1.75 \AA . Broadening of the higher J lines in the P and R branches of the $\Pi\text{--}\Pi$ subband is proposed to be due to asymmetry type doubling, the magnitude of which is consistent with the calculated barrier to H_2 internal rotation. The lower J lines in the $\Sigma\text{--}\Sigma$ and $\Pi\text{--}\Pi$ subbands have widths of 0.06 cm^{-1} , around three times larger than the laser bandwidth, corresponding to a decay time of $\approx 90\text{ ps}$ for the upper level. The absence of discernible rotational structure in the ν_2 band suggests that it has predissociation lifetime of less than 1 ps . © 1995 American Institute of Physics.

I. INTRODUCTION

Interest in the isomeric forms of H_3CO^+ followed the proposal by Herbst and Klempner in 1973 that formaldehyde may be produced in dark interstellar clouds through a mechanism in which the primary step was the radiative association of H_2 and HCO^+ .¹ The association product was presumed to be protonated formaldehyde which produced formaldehyde after dissociative recombination with electrons. Fehsenfeld, Dunkin, and Ferguson subsequently showed that H_3CO^+ ions formed in such low energy encounters rapidly exchange H_2 for CO to form $(\text{CO})_2\text{H}^+$, suggesting that they have an $\text{H}_2\text{-HCO}^+$ form, rather than the more stable protonated formaldehyde structure,² a conjecture given firm foundation by high pressure mass spectrometry measurements, which provided an association energy for the complex of $\approx 3.9\text{ kcal/mol}$ with respect to the H_2+HCO^+ limit.³ Corresponding theoretical studies^{4–10} have since identified at least three stable isomers of H_3CO^+ , the protonated formaldehyde cation H_2COH^+ which is in fact the most stable form, and the two proton bound complexes $\text{H}_2\text{-HCO}^+$ and $\text{H}_2\text{-HOC}^+$. Barriers for isomerization between the three forms appear to exceed the H_3^++CO and H_2+HCO^+ dissociation limit making it appropriate to think of them as distinct molecular species. Prior to the present study only the protonated formaldehyde cation had received spectroscopic attention.¹¹

The experimental part of the current work is concerned with the $\text{H}_2\text{-HCO}^+$ complex as revealed through its predissociative infrared absorptions. Our motivation for the investigation is twofold; we wish to produce experimental data on the H_2+HCO^+ potential energy surface which can be compared with theoretical predictions, and so be used to check the accuracy of current calculations. More generally we are interested in learning about the nature of ion–neutral inter-

actions at close range—factors governing geometries, dissociation energies, and barriers for isomerization. While the last 15–20 years have witnessed exciting experimental and theoretical work that has done much to elucidate these issues for complexes involving two or more *neutral* species,^{12–14} the corresponding questions for ion–neutral complexes are only beginning to be answered. Additional impetus arises because the $\text{H}_2\text{-HCO}^+$ complex can be viewed as a stabilized intermediate for the astrophysically important $\text{H}_3^++\text{CO}\rightarrow\text{HCO}^++\text{H}_2$ protonation reaction. Largely because of its astrophysical relevance, the reaction has come under a deal of scrutiny from quantum chemists,^{5–8} much of the work being prompted by a desire to understand relative efficiencies for the formation of formyl cation (HCO^+) and less stable isoformyl cation (HOC^+) products.

Our experimental detection of $\text{H}_2\text{-HCO}^+$ vibrational transitions is grounded upon the observation of ionic photofragments from laser excited metastable vibrational levels. The use of vibrational predissociation spectroscopy as a tool for the investigation of the structures of ionic complexes was pioneered with the study of protonated hydrogen (H_2^+H)¹⁵ and water [$(\text{H}_2\text{O})_n\text{H}^+$]¹⁶ complexes. In principle, it is similar to the bolometer optothermal technique, employed so successfully for the sub-Doppler characterization of neutral van der Waals molecules.¹⁷ Vibrational predissociation spectroscopy sports the considerable advantage of facile size selectivity of the target complex, but has the drawback that ultimately the ions must be dissociated for a transition to be inferred. Whenever a single photon is employed to probe and dissociate the complex there is always the possibility that the rotational lines are homogeneously broadened, due to a strong coupling with the dissociative continuum, sometimes to the extent that the rotational structure is obscured. Although, this appears to be the case for several of the $\text{H}_2\text{-HCO}^+$ vibrational bands, fortunately there is one transi-

tion (ν_1) which features almost complete rotational resolution, allowing a determination of ground and excited state rotational and centrifugal distortion constants.

In order to guide interpretation of the H₂-HCO⁺ spectrum we have carried out *ab initio* investigations of the potential hypersurface in regions adjacent to the H₂-HCO⁺ minimum. Although existing calculations have extensively addressed binding energies, isomerization barriers and structures of the various H₃CO⁺ isomers they have, apart from an earlier study,⁴ largely ignored vibrational properties. We focus not only on the structures and energies of H₂-HCO⁺ minima and transition states, but also determine effective approximate potentials for the intermolecular stretch vibration and H₂ internal rotation.

The spectroscopic investigations described in the present paper complement many earlier studies of neutral complexes involving the H₂ molecule, including H₂-Ar, H₂-Kr, H₄-Xe.¹⁸ Comparisons can be drawn between the properties of H₂-HCO⁺ with the ones of H₂-HF¹⁹ and D₂-HF.²⁰ In both cases the structural attributes should be strongly influenced by electrostatic forces favouring in both cases a T-shaped geometry. For H₂-HCO⁺ the leading term is a charge-quadrupole interaction while for H₂-HF it is a dipole-quadrupole term. Lovejoy, Nelson, and Nesbitt in their work on infrared transitions in the H₂-HF¹⁹ and D₂-HF²⁰ complexes observed asymmetry splittings which were an order of magnitude larger than the ones expected for a rigid rotor composed of undistorted H₂ and HF subunits. Their subsequent analysis showed that the anomalous splittings were due to large angular excursions of the H₂ subunit, the internal rotation being incompletely quenched by the anisotropic barriers. Using a simple hindered rotor Hamiltonian they were able to fit the observed splittings and infer details of the internal rotational barriers in the ground and excited vibrational states. Although efforts to pursue a similar course in the analysis of the H₂-HCO⁺ spectrum are hampered by predissociation induced line broadening, a *J* dependence in the widths provides some evidence concerning the magnitude of the anisotropy. In addition, we are able to conduct a radial analysis to obtain information on the effective rotational and centrifugal distortion constants for ground and excited vibrational states. In an H₂-HCO⁺ complex composed of largely undistorted H₂ and HCO⁺ subunits these properties are closely related to the length and strength of the H₂⋯HCO⁺ intermolecular bond. These data along with the shifts in the frequencies of the intramolecular vibrations provide direct impressions of the molecular consequences of close range ion-neutral interaction.

II. EXPERIMENTAL METHODS

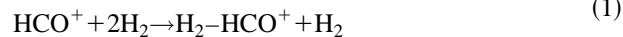
Infrared spectra of mass selected H₂-HCO⁺ complexes were obtained by exciting predissociative transitions whilst measuring the HCO⁺ fragment ion current. The quadrupole-octopole-quadrupole tandem mass spectrometer instrument used to prepare and isolate the complexes has been described previously²¹⁻²³ and here remarks are confined to essential details. In summary, ions created by an electron impact/supersonic expansion ion source are extracted and mass selected by a quadrupole mass filter before being deflected

through 90° and injected into an octopole ion guide. There they are subjected to the pulsed IR output of a two stage, tuneable optical parametric oscillator. A second quadrupole mass filter is tuned to transmit photofragment ions which are subsequently assayed with a Daly scintillation detector²⁴ coupled to boxcar integrator. Spectra are recorded by measuring the fragment current as the OPO output is scanned in frequency. The ions pass through the octopole with an energy of 8 eV, necessitating a small Doppler correction to the measured wavenumbers (+0.097 cm⁻¹ at 4060 cm⁻¹). By using the octopole ion guide as a retarding field energy analyzer an energy spread of ±1 eV was determined for the primary ion beam, implying an approximate 0.006 cm⁻¹ Doppler width for transitions near 4000 cm⁻¹.

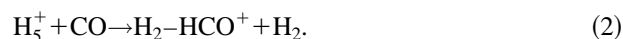
The IR light source is a tuneable, seeded, optical parametric oscillator capable of producing 500 MHz bandwidth light in the 1.5–4.0 μm range. The device possesses three stages—a master oscillator, and two amplifier/converter stages—all using KTP crystals pumped either by the 1064 nm fundamental or 532 doubled output of a seeded Nd:YAG laser. Narrow band light from the 532 nm pumped master oscillator seeds a power oscillator stage consisting of contrarotating KTP crystals pumped by the doubled output of a Nd:YAG laser (532 nm). The idler wave (first output) from this stage is introduced into a further parametric amplifier, again consisting of contrarotating KTP crystals but this time pumped by the 1064 nm Nd:YAG fundamental. The output of this stage (second output) is tuneable in the 2500–4200 cm⁻¹ range with a 0.02 cm⁻¹ bandwidth. Calibration of rotational lines in the H₂-HCO⁺ ν_1 band was achieved by simultaneously recording optoacoustic spectra of either acetylene (excited by the second OPO output) or water vapor (excited by the first output).

The ion source consists of pulsed supersonic expansion with twin electron emitting filaments positioned close to the nozzle orifice. Previous studies have shown that the source is capable of producing ionic complexes with rotational temperatures in the 30–40 K range, although on occasion the vibrational temperature can be considerably higher. In the present experiment a 15:1 mixture of H₂/CO was passed through an acetone/dry ice cooled trap to remove water vapor and expanded at 4–5 atm. An on-line computer controlled gas mixing system provides flexibility in optimizing the mixture. Adjustment of source conditions to produce H₂-HCO⁺ was achieved initially by introducing Ar or He buffer gas into the octopole region and monitoring the collision induced fragmentation into HCO⁺. Subsequently, the photofragmentation signal was maximized with the laser tuned to a resonance.

Several reaction schemes appear capable of producing H₂-HCO⁺ in the supersonic plasma, including three body association of the HCO⁺ ion with H₂ molecules



and direct formation through the reaction of H₃⁺ (or H₉⁺, etc.) with CO, e.g.,



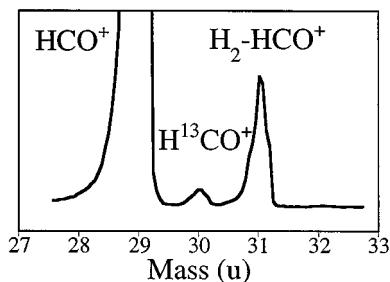


FIG. 1. Mass spectrum of ions produced in the 25–35 u range by the pulsed supersonic expansion electron impact ion source. The dominant peak at 29 u is due to HCO^+ , the one at 30 u to $\text{DCO}^+/\text{H}^{13}\text{CO}^+$, and the one at 31 u to $\text{H}_2\text{-HCO}^+$. Clear mass separation enables the attribution of photodissociation peaks to a species of one particular mass.

In fact, the second reaction scheme can be viewed as a variant of the first, in which the third body necessary for the stabilization is provided by the H_3^+ reactant.

A mass spectrum of ions produced in the 25–35 u range is shown in Fig. 1. Adjacent to the dominant HCO^+ mass peak (29 u) are smaller peaks due to $\text{H}^{13}\text{CO}^+/\text{DCO}^+$ (30 u) and H_3CO^+ (31 u). Although previous experimental²⁵ and theoretical^{4–10} works demonstrate that H_3CO^+ can exist in a number of isomeric forms including $\text{H}_2\text{-HCO}^+$, $\text{H}_2\text{-HOC}^+$, and H_2COH^+ (protonated formaldehyde), several pieces of evidence encourage the attribution of the spectra recorded in the present work to the $\text{H}_2\cdots\text{HCO}^+$ ion–neutral complex.

(1) The magnitude of the H_3CO^+ mass peak was found to be sensitive to the position of the nozzle with respect to the two electron emitting filaments, being maximized when the filaments were reasonably close to the nozzle orifice. Previous experience with the formation and spectroscopic characterization of weakly bound ionic clusters (e.g., $\text{N}_2^+\text{-He}$ ^{23,26}), leads us to take this as a sign that the molecule or complex is probably weakly bound, and requires relatively high gas densities for its formation.

(2)–Collisional dissociation of the H_3CO^+ by helium buffer gas in the octopole at 2–5 eV laboratory energy resulted in the appearance of a mass 29 peak (HCO^+ or HOC^+), strongly suggesting that a substantial fraction of the mass 31 signal is due either to $\text{H}_2\text{-HCO}^+$ or $\text{H}_2\text{-HOC}^+$. Experimental and theoretical studies indicate that although the protonation of CO by H_3^+ produces both the isoformyl HOC^+ and formyl HCO^+ species,^{27,28} the former are readily

converted to the latter through subsequent collisions with H_2 or CO .^{4,25} Given the large CO and H_2 densities in our ion source, it is likely that practically complete conversion of the isoformyl to the more stable formyl ion should occur.

(3) Finally we note that rotational constants extracted from the spectral analysis (see Sec. IV) agree with theoretical predictions for the $\text{H}_2\text{-HCO}^+$ complex, but not for the other possible isomers (see Table I).

III. CALCULATIONS

A. *Ab initio* calculations

The considerably higher proton affinity of CO compared to H_2 means that the $\text{H}_2\text{-HCO}^+$ complex can be considered essentially as an H_2 molecule associated with an HCO^+ cation. Although in principle it is possible to build up a potential energy surface describing the interaction of H_2 and CO subunits by means of *ab initio* quantum chemical methods, a degree of insight can be had simply by examining the long range electrostatic and inductive interactions. The chief attractive long range forces arise from the electrostatic interaction between the positive charge on the HCO^+ (principally localized on the H and C atoms) and the quadrupole moment of the H_2 molecule, together with the inductive charge-induced dipole interaction. That is,

$$V_{lr}(R, \theta) = \frac{Q\Theta}{8\pi\epsilon_0 R^3} (3 \cos^2 \theta - 1) - \frac{1}{2} \frac{Q^2(\alpha_{\parallel} \cos^2 \theta + \alpha_{\perp} \sin^2 \theta)}{4\pi\epsilon_0 R^4}. \quad (3)$$

[Here, Q is the ion charge, R the distance between the H_2 center of mass and the ion, α_{\parallel} and α_{\perp} the parallel and perpendicular volume polarizabilities of H_2 (0.79 and 0.93 \AA^3 , respectively²⁹), and Θ the quadrupole moment of H_2 ($+2.12 \times 10^{-40} \text{ Cm}^2$ ³⁰)]. While the induction contribution is attractive for any geometrical arrangement, the charge–quadrupole interaction may be either attractive or repulsive depending upon the orientation. In Fig. 2 the sum of the charge–quadrupole and charge-induced dipole terms are plotted as a function of separation and angle assuming that the center of mass of the H_2 lies on the HCO^+ axis. It can be seen that at intermediate ranges the total interaction is con-

TABLE I. Predicted and measured rotational constants (in cm^{-1}) for various isomers of H_3CO^+ . Calculated constants are equilibrium values while the experimental ones are vibrationally averaged.

	$\text{H}_2\text{COH}^{\text{a}}$	$\text{H}_2\text{-HOC}^{\text{b}}$	$\text{H}_2\text{-HCO}^{\text{c}}$	$\text{H}_2\text{-HCO}^{\text{d}}$	$\text{H}_2\text{-HCO}^{\text{e}}$	$\text{H}_2\text{-HCO}^{\text{f}}$
<i>A</i>	6.5903	55.1403	59.4693	60.9168	59.8183	
<i>B</i>	1.1459	0.6471	0.4763	0.4992	0.5042	
<i>C</i>	0.9730	0.6396	0.4725	0.4951	0.4999	
$\bar{B} = (B + C)/2$	1.0595	0.6434	0.4744	0.4972	0.5020	0.4872

^aExpt. Reference 11.

^bCalc. Reference 6.

^cCalc. Reference 7.

^dCalc. Reference 8.

^eCalc. present work.

^fExpt. B_0 value obtained from analysis of the ν_1 $\Pi\text{-}\Pi$ subband.

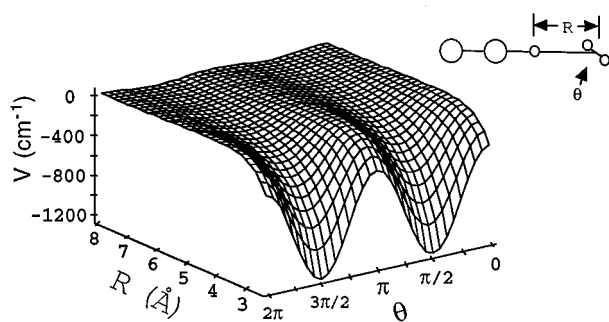


FIG. 2. Electrostatic and induction $\text{H}_2\cdots\text{HCO}^+$ interaction potential [Eq. (3)] with parameters as described in the text. Long range charge-quadrupole interactions favor a T-shaped configuration, although due to the attractive inductive contribution the linear configuration is also stable at smaller intermolecular separations.

siderably more attractive in the T-shaped than the linear configuration, leading one to anticipate a substantial barrier to the internal rotation of the H_2 molecule.

In order to better understand the nature of the $\text{H}_2\text{-HCO}^+$ complex, equilibrium geometries, potential energy curves, harmonic force fields and dissociation energies were calculated using the GAUSSIAN 92 programs.³¹ The approach involved using the quadratic configuration interaction method, including all single and double excitations from single determinant, self-consistent field (SCF) wave functions (QCISD).³² Effects of connected triple excitations were added to the QCISD energies in a perturbative way using the QCISD(T) approach. Although in principle the latter method offers improved accuracy over the QCISD wave function, it is slightly cumbersome as analytical gradients are not readily available. For this reason, the majority of data presented here are the result of purely numerical methods based on energy only minimisation in the case of equilibrium geometry location, and numerical construction of a quadratic Hessian in the case of the harmonic force field calculations.

Two Gaussian basis sets were used for this work. Harmonic frequencies were calculated using the 6-311G(*d,p*) basis of Pople and co-workers.³³ Refined equilibrium structures, energies, and potential energy functions were calculated using the more flexible 6-311G(2*df*,2*pd*) basis set. At the highest level of theory [QCISD(T)/6-311G(2*df*,2*pd*)], the equilibrium structures of the monomeric units H_2 and HCO^+ were in close agreement to the experimental observations. The internuclear distance for H_2 was 0.743 Å and for HCO^+ , $r_{\text{(CH)}}=1.093$ Å and $r_{\text{(CO)}}=1.112$ Å (exp; $r_{\text{e(CH)}}=1.097$ Å, $r_{\text{e(CO)}}=1.105$ Å³⁴). Comparisons reveal that the calculated harmonic frequencies overestimate the molecular vibrational spacings. Thus for the ν_1 mode of HCO^+ the calculated value (3238 cm^{-1}) is around 150 cm^{-1} higher than the observed one (3088.727 cm^{-1}). For the H_2 stretch the calculated value was 4402 cm^{-1} , approximately 5.8% larger than the experimental first vibrational spacing (4161 cm^{-1} ³⁵).

For $\text{H}_2\text{-HCO}^+$ a survey of the ion-molecule complex potential energy surface revealed two stable conformers with C_{2v} and C_s symmetries. The lower energy C_{2v} structure

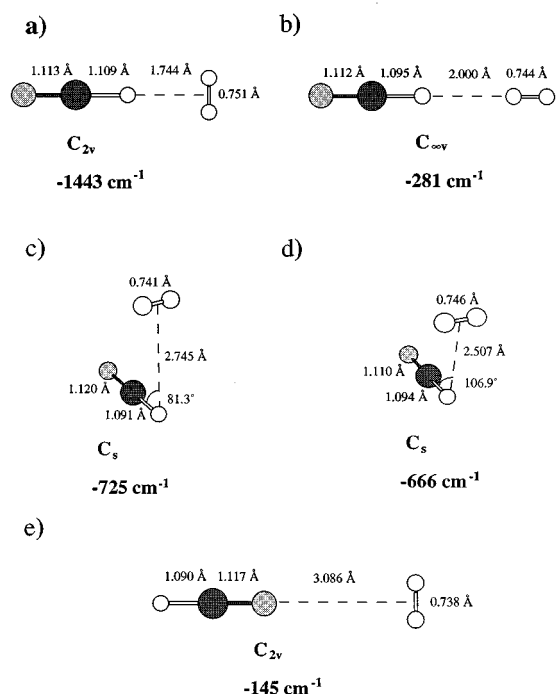


FIG. 3. Stationary points on the $\text{H}_2\text{-HCO}^+$ hypersurface, with energies determined at the QCISD(T)/6-311G(2*df*,2*pd*) level. Energies with respect to the H_2+HCO^+ dissociation limit are given in brackets next to each structure. The transition state between the C_{2v} and C_s minima was located at the QCISD/6-311G(*d,p*) level of theory with a subsequent energy calculation at the QCISD(T)/6-311G(2*df*,2*pd*) level. Although the C_{2v} T-shaped structure (a) is the global minimum there is also a secondary C_s minimum (c).

[Fig. 3(a)] is stabilized by 1443 cm^{-1} with respect to H_2+HCO^+ (neglecting zero point energy), and has been identified in several previous theoretical studies. The C_s conformer [Fig. 3(c)] lies -725 cm^{-1} below the dissociation limit, and is separated from the C_{2v} minimum by a 59 cm^{-1} barrier [Fig. 3(d)]. The calculations show that the C_{2v} conformer lies 4.13 kcal/mol lower in energy than the separated monomeric units, or 2.43 kcal/mol when harmonic, zero point energy corrections are taken into account. Although the $\text{H}_2\text{-HCO}^+$ bond energy, the heat of formation at 300 K has been determined to be -3.9 kcal/mol. After standard thermodynamical corrections are made to the theoretical result,³⁶ the ΔH_{300}^0 for the ion-molecule reaction becomes -3.19 kcal/mol, representing a reasonable agreement with the experimental value.³

B. Vibrations of $\text{H}_2\text{-HCO}^+$

In order to establish contact between the *ab initio* calculations and the experimental spectrum it is necessary to determine vibrational frequencies and transition strengths. Harmonic vibrational frequencies and dipole strengths for the nine normal vibrational modes of the $\text{H}_2\text{-HCO}^+$ complex determined in conjunction with the *ab initio* calculations described above, along with symmetries and descriptions are listed in Table II and illustrated in Fig. 4. One expects that in a moderately bound complex such as $\text{H}_2\text{-HCO}^+$ the vibrations should factor into high frequency ones involving inter-

TABLE II. Symmetries, vibrational frequencies, and transition dipole strengths ($|\langle 0|\mu|f\rangle|^2$) for the H₂-HCO⁺ complex. Frequencies and dipole strengths were determined in conjunction with the *ab initio* calculations. The frequencies given in brackets have been scaled by the factor necessary to bring the corresponding monomer (HCO⁺, H₂) calculated and observed frequencies into line. Normal modes are illustrated in Fig. 4.

Mode	Symmetry	Description	Frequency (calc) (cm ⁻¹)	Frequency (expt) (cm ⁻¹)	$ \langle 0 \mu f\rangle ^2$ ($\times 10^{-1}$ D ²)
1	<i>a</i> ₁	H-H stretch	4324 (4073)	4060	0.48
2	<i>a</i> ₁	C-H stretch	2990 (2850)	2840	9.3
3	<i>a</i> ₁	C-O stretch	2168 (2139)		5.4
4	<i>a</i> ₁	H ₂ ···HCO stretch	353	305 ^a 300 ^b	5.4
5	<i>b</i> ₁	HCO ⁺ out of plane bend	956 (1034)		0.35
6	<i>b</i> ₁	low frequency out-of-plane bend	197	(39) ^c	4.2
7	<i>b</i> ₂	HCO ⁺ in-plane bend	973 (1053)		0.24
8	<i>b</i> ₂	H ₂ rock	608		0.70
9	<i>b</i> ₂	low frequency in-plane bend	195	(36) ^d	5.0

^aAssuming that the 3145 cm⁻¹ band is $\nu_2 + \nu_4$.

^bDerived from measured centrifugal distortion constants.

^cAssuming that 2879.08 band is $\nu_2 + \nu_6$.

^dAssuming that 2876.36 band is $\nu_2 + \nu_9$.

nal deformations of the molecular subunits shown at the top of Fig. 4 (H₂ stretch and HCO⁺ stretches and bends), and ones of lower frequency involving “intermolecular” motions (shown at the bottom of Fig. 4). Vibrations in the former category should be similar in nature to the ones of the isolated subunits although, depending upon the strength of the intermolecular interactions frequencies will be shifted somewhat. It is easy to identify the ν_1 vibration of H₂-HCO⁺ with the H₂ stretch, ν_2 and ν_3 with the C-H and C-O stretches of HCO⁺, and ν_5 and ν_7 with the HCO⁺ degenerate bend. In order to better predict the intermolecular frequencies of the H₂-HCO⁺ complex, the calculated values were scaled by a factor necessary to bring the corresponding monomer calculated frequencies into line with the experimental ones. These scaled frequencies are also provided in Table II and are the ones given in Fig. 4.

Besides vibrations involving deformations of the complexes' constituents there are four intermolecular vibrations—the stretching vibration of the H₂···HCO⁺ bond (ν_4), an H₂ rocking vibration (ν_8) and two bending vibrations which principally entail in-plane and out-of-plane motion of the H₂ unit (ν_9 and ν_6). Regarding these *intermolecular* vibrations as a collection of normal modes may not be a good approximation. Flat intermolecular potential energy surfaces and small reduced masses imply substantial vibrational displacements and thus exploration of the PES well away from the minimum. In order to investigate anharmonic effects for the intermolecular stretching and bending motions, a series of potential energy points away from the minimum energy configuration were calculated. For the intermolecular stretch, an effective *ab initio* stretching potential was determined by calculating the energy at a number of different intermolecu-

lar bond separations, all other degrees of freedom being allowed to relax. The resulting potential is illustrated in Fig. 5. Equipped with this potential the radial Schrödinger equation was solved numerically to yield vibrational energy levels.³⁷ This calculational strategy presumes effective decoupling between intermolecular stretch and the other molecular motions. As expected the first vibrational spacing for the intermolecular stretch potential shown in Fig. 5 (320 cm⁻¹) is somewhat lower than the corresponding harmonic frequency (353 cm⁻¹).

Analysis of the large amplitude intermolecular bending motions is more complicated. In the limit of negligible steric hindrance the three bending vibrations will correlate to internal rotations—the H₂ rock with internal rotation of the H₂, and the two low frequency bends with an internal rotation of the HCO⁺ ion. The two internal rotational motions will be coupled to some extent by cross terms in the potential energy expansion, so that if one really wishes to understand the full problem it is necessary to treat the two motions simultaneously. At this stage our experimental spectra are not sufficiently detailed to warrant a complete analysis of the coupled bending problem, and in this paper we confine discussion to a qualitative examination of the nature of the H₂ internal rotation considered in isolation from the other low frequency motions.

Some insight into the character of the H₂ rock/internal rotation can be derived by considering a simple atom-diatom hindered rotor Hamiltonian, useful discussions of which can be found in Refs. 19 and 38. Neglecting the radial motion and pretending for the moment that the HCO⁺ can be thought of as a point mass, the Hamiltonian for a hindered

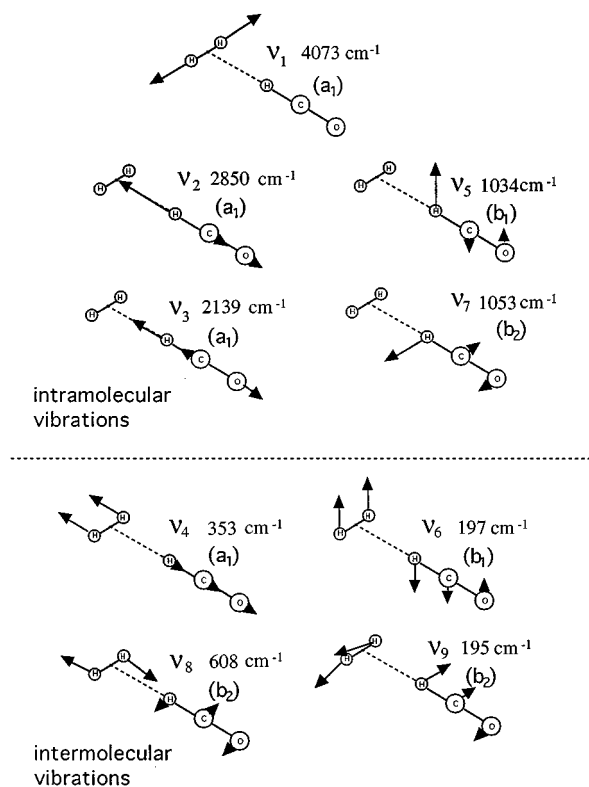


FIG. 4. Normal modes of H₂-HCO⁺ determined in conjunction with the quantum chemical calculations described in Sec. III. The modes factor into five intramolecular vibrations (illustrated at the top of the figure) and four lower frequency intermolecular vibrations (shown at the bottom). While the normal frequencies for the intramolecular modes are likely to be reasonably close to the experimental values, the intermolecular motions are expected to have large amplitude, anharmonic character and the normal mode frequencies may be in substantial error. The frequency for each intramolecular motion has been scaled by the factor necessary to bring the corresponding monomer unit calculated and observed frequency into line (see the text).

rotor atom-diatom molecule can be written in a space fixed coordinate system as

$$\hat{H} = b\hat{\mathbf{j}}^2 + B\hat{\mathbf{I}}^2 + V(\theta), \quad (4)$$

where $\hat{\mathbf{j}}$ and $\hat{\mathbf{I}}$ are angular momentum operators pertaining, respectively, to the rotation of the diatomic (rotational constant b) and of the entire complex (rotational constant B). Usually the potential function $V(\theta)$ is expanded in a sum of Legendre polynomials in $\cos \theta$,

$$V(\theta) = \sum_{\lambda} V_{\lambda} P_{\lambda}(\cos \theta), \quad (5)$$

where θ is the angle between the diatomic bond and the line joining the diatomic center of mass and the atom. As the total angular momentum of the system is conserved, it is convenient to expand the eigenfunctions of the Hamiltonian in terms of basis functions that are simultaneous eigenfunctions of $\hat{\mathbf{j}}^2$, $\hat{\mathbf{I}}^2$, $\hat{\mathbf{J}}^2$, and $\hat{\mathbf{J}}_z$ (where $\hat{\mathbf{J}}$ is the total angular momentum operator; $\hat{\mathbf{J}} = \hat{\mathbf{j}} + \hat{\mathbf{I}}$). Such a basis can be constructed as the sum of spherical harmonic products

$$\psi_{jl}^{JM} = \sum_{m_j m_l} \langle jlm_j m_l | JM \rangle Y_{jm_j} Y_{lm_l}, \quad (6)$$

where the $\langle jlm_j m_l | JM \rangle$ are Clebsch-Gordan coefficients. Matrix elements of the space fixed Hamiltonian (4) with the basis set (6) are given in Refs. 19 and 38. For a homonuclear diatomic only even potential terms need be considered and the problem separates into ones involving even and odd j terms.

Although strictly only the total angular momentum J , and the parity $p' = (-)^{j+1}$ are good quantum numbers, depending upon the magnitude of the hindering potential other quantum numbers are approximately good. In the limit of an isotropic potential [$V(\theta) = 0$], j and l are both good quantum numbers and the two rotations are decoupled from one another. However, as $V(\theta)$ increases, the internal rotation becomes coupled to the end-over-end tumbling and l ceases to be good quantum numbers although for moderate hindering potentials, j and its projection on the intermolecular axis K remain approximately good. Eventually, when $V(\theta)$ becomes large enough, the system effectively becomes a semi-rigid near prolate symmetric top [$V(\theta) > 0$] or linear molecule [for $V(\theta) < 0$]. Transitions between the various regimes have been discussed in the literature,³⁸ and depend upon the ratio of the anisotropy to the diatomic rotational constant, so that for a diatomic with a large rotational constant such as H₂ ($B \approx 60$ cm⁻¹), considerable barriers are necessary to quench the internal rotation.

Several points should be emphasized. First of all, when the $P_2(\cos \theta)$ term dominates the potential expansion, for any particular K manifold the level spacings are approximately as they are for a diatomic molecule

$$E(K, J) = E_K + B_{\text{eff}} J(J+1) (J \geq K) \quad (7)$$

although the spacings between the different K manifolds are not as expected for a prolate symmetric top (except in the limit of very high V_2). This has the consequence that if the

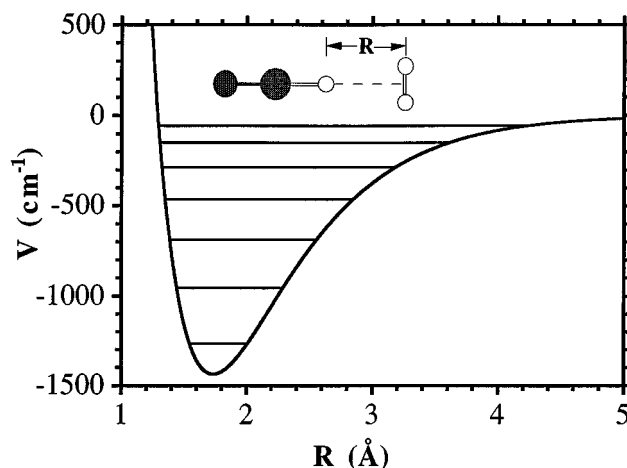


FIG. 5. Intermolecular stretching potential for H₂-HCO⁺, determined by varying the H₂···HCO⁺ intermolecular separation while allowing all other degrees of freedom to relax. Vibrational level spacings were determined by numerically solving the radial Schrödinger equation (Ref. 37).

TABLE III. Energies of $\text{H}_2\text{-HCO}^+$ configurations where the H_2 bond is tilted by an angle of α with respect to the HCO^+ bond, the H_2 center of mass being constrained to lie on the HCO^+ axis, and all other molecular degrees of freedom being allowed to relax. Zero energy is taken to be at $\alpha=90^\circ$ (T-shaped configuration). A Legendre sum potential [Eq. (5)] fitted to these points is shown in Fig. 6.

α (degrees)	Energy (cm^{-1})
0	1162
10	1145
30	969
80	70
90	0

symmetry of the transition is such that a $\Delta K=0$ selection rule applies, the spectrum will appear as a collection of diatomic like overlapping subbands each characterized by a different K value. Second, for $K>0$ there are $p' = (-)^{j+1} = +1$ and -1 parity levels for each J , the energetic disposition of which for low J can be represented by Eq. (7) with slightly different effective rotational constants. The splitting is largest for $K=1$ states, and depends sensitively upon the size of the anisotropic terms in the potential, manifesting itself in the P and R branch of a parallel infrared band with pairs of transitions which are displaced slightly from one another, in much the same way as asymmetry doublets of a near prolate symmetric top. The splitting *increases* markedly as the barrier to internal rotation *decreases*, and thus as demonstrated by Lovejoy and Nesbitt in their study of the $\text{H}_2\text{-HF}^{19}$ and $\text{D}_2\text{-HF}^{20}$ complexes, can be used to diagnose the magnitude of the steric hindrance.

An approximate effective potential for the H_2 rocking motion was determined by calculating the complexes' energy with the H-H bond tilted at angles of 0, 10, 30, 60, 80, and 90 deg with respect to the HCO^+ axis (the H_2 center of mass being constrained to lie on the HCO^+ axis), all other molecular degrees of freedom being allowed to relax at each angular point. The resulting energies (given in Table III) were used to find least squares values for the first two even coefficients in the Legendre expansion for the potential [Eq. (5)], yielding $V_2=818 \text{ cm}^{-1}$ and $V_4=-118 \text{ cm}^{-1}$ (taking the bottom of the angular well to be $V=0$). Here, we ignore coupling between the internal rotation and intermolecular stretching coordinates, perhaps not an inconsiderable effect as comparison of Figs. 3(a) and 3(b) shows, with a substantially longer H- H_2 bond in the linear configuration than in the T-shaped one. Equipped with the angular potential, the hindered rotor Hamiltonian was diagonalized using the basis (6) to yield eigenvalues and eigenvectors. The b and B rotational constants were taken as the ones for hydrogen in its ground vibrational state ($b_0=59.322 \text{ cm}^{-1}$) and the calculated equilibrium one for $\text{H}_2\text{-HCO}^+$ ($B_e=0.502 \text{ cm}^{-1}$). A basis including j values up to 13 was used, sufficient to converge the lower level eigenvalues to less than 0.001 cm^{-1} .

The lowest rotational levels of the first few K manifolds are shown in Fig. 6. As mentioned above, wave functions of even and odd j parentage are not mixed by the potential, and thus there are independent ortho (j odd) and para (j even) modifications of $\text{H}_2\text{-HCO}^+$ which should exist in 3:1 popu-

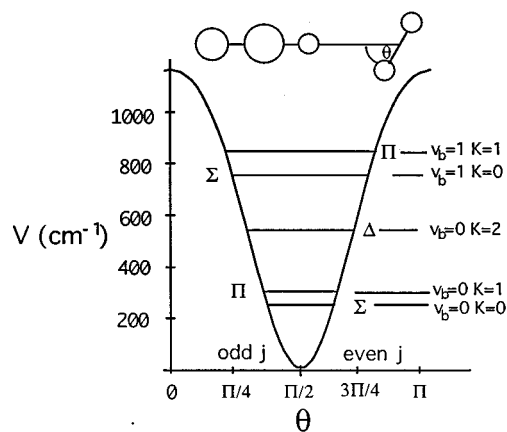


FIG. 6. *Ab initio* H_2 rocking potential for $\text{H}_2\text{-HCO}^+$ determined by varying the angle between the intermolecular and H_2 axes while allowing all other degrees of freedom to relax. The energy levels have been calculated using by diagonalizing the space fixed Hamiltonian [Eq. (4)]. Levels with even (odd) j parentage are indicated by a symmetry label on the right (left) of the potential curve. Given on the far right are the T-shaped rigid rotor designations (v_b =bending quantum number, K =projection of total angular momentum on the intermolecular axis). Only the lower two K manifolds are populated in the experiments described here.

lation ratio. Symmetries of the states deriving from even and odd j combinations are shown, respectively, on the right and left of the potential. It is possible to correlate the two lower levels with those of a T-shaped prolate top with quantum numbers $v_b=0$ for the bending vibration and K for the projection of the angular momentum onto the intermolecular axis. This is done on the right side of Fig. 6. In fact as a consequence of the relatively large hindering potential the spacing between the lowest two levels ($v_b=0 K=0$ and $v_b=0 K=1$) is quite close to the one expected for a prolate symmetric top (69 cm^{-1} compared to 59.322 cm^{-1}). By fitting the bottom few J levels of the $p' = +1$ and -1 manifolds of the lowest $K=1$ level we derive effective rotational constants of 0.5018 and 0.4983 cm^{-1} respectively, implying a J dependent splitting in the P and R branch transitions which increases approximately as $J \times 0.007 \text{ cm}^{-1}$.

What clues can we hope to find in the $\text{H}_2\text{-HCO}^+$ spectrum concerning the size of the barrier for H_2 internal rotation? In principle, we could learn most about the barrier by measuring the spacing between the different K manifolds shown in Fig. 6. However, in practice, because of the relatively low temperature of our ions (30–40 K), it is only lower two K manifolds ($v_b=0 K=0$) and ($v_b=0 K=1$) that are appreciably populated. Furthermore, the only band displaying resolved rotational features is a parallel one, so that we are confined to observing $\Delta K=0$ $\Sigma\text{-}\Sigma$ and $\Pi\text{-}\Pi$ subbands. Under these circumstances the primary source of evidence for the magnitude of the H_2 internal rotation barrier comes from the J dependent splitting in the $\Pi\text{-}\Pi$ subband.

The other two low frequency bending motions which involve motion of the H_2 unit about the HCO^+ (ν_6 and ν_9 in Fig. 4), are also likely to entail substantial excursions from the equilibrium configuration. For the lower vibrational levels it is likely that the out of plane ν_6 and in plane ν_9 vibrations will be quasidegenerate. To a first approximation, the

problem can be approached in the same way as for the H_2 rock/internal rotation, in this case by considering the HCO^+ molecule as a diatomic and the H_2 molecule as an atom, although because of the rather small rotational constant of HCO^+ ($\approx 1.5 \text{ cm}^{-1}$), lesser barriers are required to quench the internal rotation than for the H_2 rocking motion. The *ab initio* calculations suggest that the barrier for circumnavigation of the H_2 about the HCO^+ is of the order of 1300 cm^{-1} , much greater than the HCO^+ rotational constant ($b_e \approx 1.5 \text{ cm}^{-1}$) and thus in contrast to the H_2 rocking motion, the internal rotation should be effectively quenched, so that at least for the lower vibrational levels the two bends should be approximately harmonic.

IV. RESULTS AND ANALYSIS

A. Vibrational band assignments

Assignment and analysis of the vibrational band structure is based largely on the expectation that complexation of H_2 and HCO^+ will not greatly perturb the intramolecular vibrational frequencies and also upon the *ab initio* and normal coordinate calculations described in the preceding section. The vibrational predissociation spectrum of $\text{H}_2\text{-HCO}^+$ in the $2500\text{--}4500 \text{ cm}^{-1}$ range is shown in Fig. 7. Although the spectrum appears at first sight to consist only of two major bands centered near 2840 and 4060 cm^{-1} , closer examination reveals that the 2840 cm^{-1} system is in fact composed of three close lying transitions (Fig. 8) and that the 4060 cm^{-1} system (Fig. 9) is comprised of two overlapping bands. In addition a very weak band appears at around 3145 cm^{-1} . Positions, structures and assignments of the different vibrational bands are given in Table IV.

Considering the part of the spectrum lying between 2800 and 2900 cm^{-1} first, we note that three band systems can be distinguished, none exhibiting resolved rotational lines. The most intense of the three is the one to lower energy at 2840 cm^{-1} . Its strength and wave number immediately encourage one to assign it as due to excitation of the CH stretching fundamental of the HCO^+ subunit, consistent with the calculations (Sec. III) which predict the occurrence of a strong

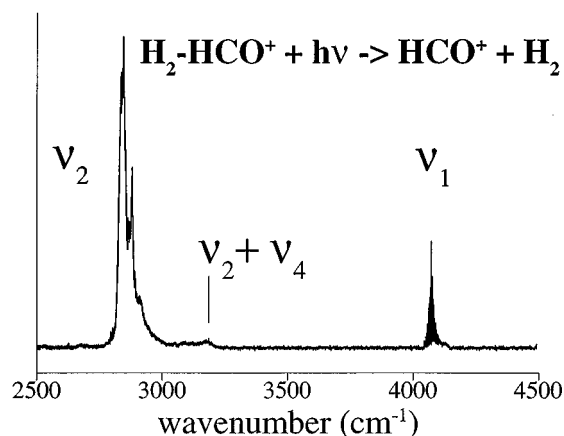


FIG. 7. Vibrational predissociation spectrum of $\text{H}_2\text{-HCO}^+$ in the $2500\text{--}4500 \text{ cm}^{-1}$ range recorded by monitoring the HCO^+ photoyield. Band assignments and wave numbers are given in Table IV.

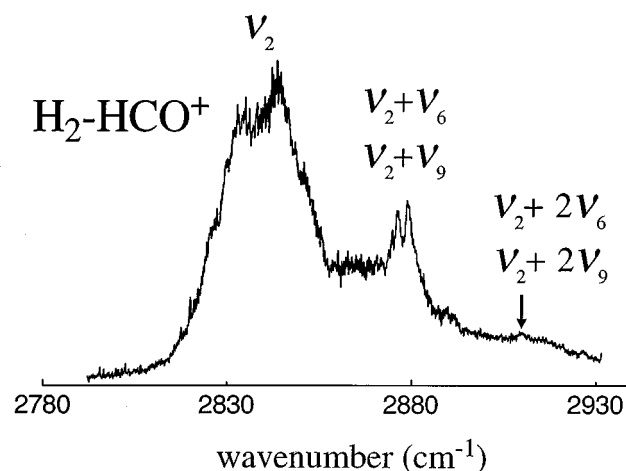


FIG. 8. Expanded view of the 2840 cm^{-1} system, composed of the ν_2 and $\nu_2 + \nu_6$ and $\nu_2 + \nu_9$ bands.

band at 2850 cm^{-1} (Fig. 4, Table II). Such an assignment is also consistent with its rather broad ($\approx 40 \text{ cm}^{-1}$ FWHM) structure, suggestive of a parallel transition of a prolate symmetric top. The two higher lying bands are somewhat sharper, and are separated by only around 3 cm^{-1} (2876.4 and 2879.1 cm^{-1}). Their close spacing and rather sharp structure, indicative of the Q branches of perpendicular transitions, leads one to suspect that they represent two close lying combination bands involving the two lowest frequency bending levels (ν_6 and ν_9) and the C–H stretch (ν_2). The normal harmonic frequencies of the two bends are only 2.5 cm^{-1} apart at 194.7 and 197.2 cm^{-1} (see Table II and Fig. 4), although if the bands in question involve the $\nu_2 + \nu_6$ and $\nu_2 + \nu_9$ combinations, the calculated harmonic frequencies must considerably overestimate the true ν_6 and ν_9 values. This is quite possible given that these two bending vibrations will have large amplitudes and should sample regions of the potential well away from the minimum. Though there are other combination bands that should also have a perpendicular structure and which should also fall in the same region (e.g., $\nu_3 + \nu_5$ and $\nu_3 + \nu_7$), the *ab initio* calculations predict these bands to be considerably weaker than the $\nu_2 + \nu_6$ and

TABLE IV. Observed vibrational band positions and assignments for $\text{H}_2\text{-HCO}^+$. The assignments are discussed in Sec. V. Harmonic normal mode motions are illustrated in Fig. 4.

Band wave number (cm^{-1})	Description	Assignment
2840	Parallel (v. strong)	ν_2
2876.36	Perpendicular (strong)	$\nu_2 + \nu_9$
2879.08	Perpendicular (strong)	$\nu_2 + \nu_6$
3145	Parallel	$\nu_2 + \nu_4$
4060.315	Parallel	ν_1 ($\Pi\text{-}\Pi$ band)
4063.822	Parallel	ν_1 ($\Sigma\text{-}\Sigma$ band)

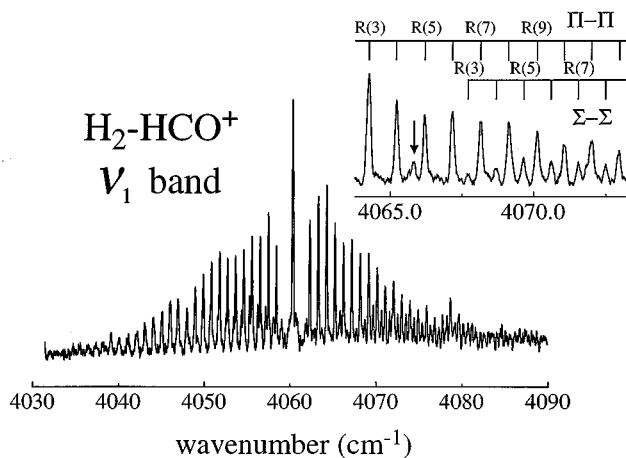


FIG. 9. Expanded view of the 4060 cm⁻¹ ν_1 band system of H₂-HCO⁺. Wave numbers for the $\Pi\leftarrow\Pi$ and $\Sigma\leftarrow\Sigma$ subbands are given in Table V. The arrow marks the position of the unidentified Q branch (see the text).

$\nu_2 + \nu_9$ combinations and to lie much further apart than 3 cm⁻¹.

Somewhat to higher in energy, at around 3145 cm⁻¹ is an extremely weak band having the appropriate wave number and structure (parallel band) for assignment to the $\nu_2 + \nu_4$ combination, that is the C-H stretch vibration in conjunction with the low frequency H₂···HCO⁺ stretch. The displacement from the ν_2 fundamental is 305 cm⁻¹ in good agreement with the value calculated for ν_4 using the effective potential shown in Fig. 5 (320 cm⁻¹).

Finally, occurring near 4060 cm⁻¹ are two weak, rotationally resolved subbands having the $\Sigma\leftarrow\Sigma$ and $\Pi\leftarrow\Pi$ structures anticipated for parallel $\Delta K=0$ subbands from $K=0$ and $K=1$ manifolds of a prolate symmetric top (Fig. 9). The two subbands occur some 100 cm⁻¹ to lower energy from the free H₂ stretch vibration (4161 cm⁻¹), and are almost indisputably associated with the ν_1 vibration of the complex. We note that the $\Sigma\leftarrow\Sigma$ subband is somewhat weaker than the $\Pi\leftarrow\Pi$ one, consistent with the nuclear spin weights for para and ortho H₂, and thus suggesting that the H₂-HCO⁺ complex contains two equivalent hydrogen atoms. Such a finding is compatible with both a T-shaped semirigid prolate symmetric top structure and also with a situation where the hydrogen molecule undergoes hindered internal rotation.

We have also observed but not properly identified a rather sharp peak occurring at 4065.76 between $R(4)$ and $R(5)$ of the $\Pi\leftarrow\Pi$ subband. The peak stands alone and appears not to belong to either the $\Sigma\leftarrow\Sigma$ and $\Pi\leftarrow\Pi$ subbands of the ν_1 transition. It might possibly consist of the overlapping Q branches of the $\nu_1 + \nu_6 - \nu_6$ and $\nu_1 + \nu_9 - \nu_9$ hot band transitions which should lie close to one another.

B. Rotational analysis of the ν_1 band

A pseudodiatomic approach to the rotational analysis of the ν_1 subband was adopted, with separate fitting of the $\Sigma\leftarrow\Sigma$ and $\Pi\leftarrow\Pi$ rotational lines (vacuum wave numbers in Table V), upper and lower state rotational levels being given

TABLE V. Rotational line wave numbers for the $\Sigma\leftarrow\Sigma$ and $\Pi\leftarrow\Pi$ subbands of the ν_1 transition of H₂-HCO⁺. Differences (last two significant figures) between measured wave numbers and ones calculated using Eq. (8) and fitted constants given in Table VI are listed after each entry.

J	$\Pi\leftarrow\Pi$ band		$\Sigma\leftarrow\Sigma$ band	
	$R(J)$	$P(J)$	$R(J)$	$P(J)$
				4060.322/-07 ^a
1	4062.274/-04			
2	63.276/-25	4058.360/08		
3	64.251/-15	57.418/-19	4067.738/01	4060.908/05
4	65.199/22	56.429/04	68.748/-22	59.938/10
5	66.183/26	55.470/-01	69.723/-09	58.978/09
6	67.191/07	54.501/07	70.708/-03	58.018/11
7	68.190/00	53.536/14	71.693/06	57.078/-03
8	69.201/-17	52.598/-03	72.683/13	56.138/-14
9	70.195/-14	51.645/-01	73.688/09	55.177/00
10	71.168/10	50.686/10	74.708/-07	54.228/06
11	72.154/23	49.759/-07	75.718/-10	53.318/-23
12	73.160/21	48.830/-19	76.703/17	52.368/-06
13	74.198/-13	47.884/-10	77.723/13	51.417/15
14	75.207/-16	46.912/30	78.778/-22	50.508/02
15	76.214/-15	45.997/16	79.778/03	
16	77.225/-15	45.099/-08		
17	78.212/10	44.170/-01		
18	79.219/18	43.248/10		
19	80.258/-03	42.357/-07		
20	81.277/02	41.474/-27		
21		40.569/-19		
22		39.627/30		

^a Q branch position.

by the formula:

$$F(J) = B_v[J(J+1) - K^2] - D_v[J(J+1) - K^2]^2 \quad (8)$$

with $K=0$ for Σ states and $K=1$ for Π states. Constants derived from the fit are given in Table VI. Due to better signal to noise ratio, parameters are more precisely determined for the $\Pi\leftarrow\Pi$ subband than for the $\Sigma\leftarrow\Sigma$ one. As well, the rather prominent Q branch makes rotational numbering for the $\Pi\leftarrow\Pi$ subband straightforward. Matters are more difficult for the $\Sigma\leftarrow\Sigma$ subband where due to the absence of a Q branch and difficulty in locating the first few P and R branch lines the numbering remains somewhat tentative. The numbering eventually adopted places the subband origin midway between the estimated intensity maxima of the P and R branches, between the $R(2)$ and $R(3)$ lines of the $\Pi\leftarrow\Pi$ transition. Inspection of Table V where the difference between the measured line positions and the ones calculated using the fitted constants inserted into Eq. (1), shows that deviations are generally of the order 0.01–0.02 cm⁻¹, somewhat less than the width of the narrower lines (0.06 cm⁻¹).

Rotational B values extracted from the analysis are close to the calculated ones (Table I), persuasive evidence that it is indeed the H₂-HCO⁺ species that we observe. We note that the $\Sigma\leftarrow\Sigma$ B values are slightly smaller than the $\Pi\leftarrow\Pi$ ones and also that the upper state B value is significantly larger than the lower state one for both subbands. Introduction of the rotational and centrifugal distortion constants listed in Table VI into the relationship³⁹

TABLE VI. Constants (in cm⁻¹) for Σ←Σ and Π←Π subbands of the H₂-HCO⁺ ν₁ transition. The constants were obtained from a least squares nonlinear fit of rotational line positions (Table V) to the pseudodiatomic expression given in Eq. (8). Values given in brackets are the 2σ uncertainties in the last two figures of the measured constants.

	Π-Π subband	Σ-Σ subband
ν ₀	4060.315(08)	4063.822(11)
B''	0.4872(04)	0.4863(06)
D''	3.54e-6(63)	2.6e-6(2.3)
B'	0.4884(04)	0.4877(06)
D'	3.18e-6(67)	1.5e-6(1.8)

$$\nu_4 = \sqrt{\frac{4B_e^3}{D} \left(1 - \frac{B_e}{B_{\text{HCO}}}\right)}$$

allows an estimate for the intermolecular stretch frequency of around 300 cm⁻¹.

In the ν₁ band, rotational linewidths are at least 0.06 cm⁻¹, approximately three times greater than the laser bandwidth (0.02 cm⁻¹) and around an order of magnitude larger than the expected doppler width (0.006 cm⁻¹, assuming an energy spread of ±1 eV in the 8 eV H₂-HCO⁺ beam). We remark that for other complexes studied using the same methods (e.g., HCO⁺-Ne), we have observed laser limited linewidths. If the broadening results from rapid predissociation, it would correspond to an upper state lifetime of around 90 ps. The absence of discernible rotational features for the bands near 2800 cm⁻¹ indicates that for these, linewidths exceed 3–5 cm⁻¹, suggesting upper state lifetimes of less than 1 ps.

V. DISCUSSION

The H₂-HCO⁺ complex is a member of a class of AHB⁺ complexes commonly known as proton bound complexes. A series of thermochemical measurements⁴⁰ shows that the stability of such species can be correlated with the difference in the proton affinities of A and B. When the difference is small, the proton is effectively shared by A and B and the binding energy is comparatively large, the archetypal example of this case being the H₅⁺ complex, whose binding energy with respect to dissociation into H₃⁺+H₂ is 9.6 kcal/mol. On the other hand, if there is a large disparity in affinities, the complex is better considered as a neutral molecule bound by electrostatic and inductive forces to a protonated molecular ion. This is likely to approximate the situation for H₂-HCO⁺ where the PA of CO (142 kcal/mol⁴¹) considerably exceeds the one of H₂ (101 kcal/mol⁴¹). Still, the cohesion of the complex remains substantial, with experimental, thermochemical measurements indicating a binding energy of the order of 3.9 kcal/mol (≈1365 cm⁻¹) with respect to HCO⁺+H₂ products.³ Thus the complex is more stable than most neutral van der Waals molecules, but less so than ionic homodimers of the type Ar₂⁺ and N₄⁺ which are typically bound by around 25 kcal/mol.⁴⁰

While it may be useful to think of H₂-HCO⁺ as merely an H₂ molecule electrostatically bound to an HCO⁺ cation, subtle effects involving transfer of electron density from one

of the moieties to the other should express themselves through small changes in the constituents' vibrational frequencies and geometries as they approach one another. Our experimental spectra of H₂-HCO⁺ provide information on two intramolecular vibrations—the H–H stretch localized on the H₂ (ν₁=4060 cm⁻¹) and the C–H stretch localized on the HCO⁺ (ν₂=2840 cm⁻¹). In both cases, comparison with the corresponding vibrations of the isolated molecules (H₂ ν₀=4161 cm⁻¹,³⁵ HCO⁺ ν₁=3089 cm⁻¹⁴²) shows that the frequency decreases upon complexation. For the H₂ stretch, a simple explanation may be that the positive charge localized on the HCO⁺ withdraws electron density from the H–H bond, thereby weakening it. In the case of the HCO⁺ part of the complex, transfer of electron density from H₂ to HCO⁺ may give the latter some HCO *neutral* character. As HCO has a somewhat lower C–H stretching frequency (2434 cm⁻¹⁴³ compared to 3089 cm⁻¹ for HCO⁺⁴²) a reduction in frequency might again be expected.

Where comparison between calculated and measured molecular properties is possible the agreement is good. Particularly satisfying is the close correspondence between computed and measured rotational constants (Table I), compelling evidence that we are indeed observing an H₂-HCO⁺ isomer with a structure much as shown in Fig. 3(a). It should be remembered that the effective B_v values determined spectroscopically are related to the vibrationally averaged value of the inverse moment of inertia, and as the bond between the H₂ and HCO⁺ ion is relatively weak, B_v values will be somewhat less than the B_e ones. We note that the calculations overestimate both the ν₁ and ν₂ intramolecular vibrational frequencies, as they also do for the corresponding motions in the monomer subunits. It is reassuring to note that almost identical proportional corrections are necessary to bring the measured and calculated H–H and C–H frequencies into line for the subunits and for the complex. For the intermolecular motions it is necessary to go beyond the harmonic approximation presuming infinitesimal displacements, and to explicitly consider the large amplitude nature of the vibrations. When this is done for the *intermolecular* stretch, with calculation of an effective *ab initio* stretch potential and solution of the radial Schrödinger equation, there is excellent agreement between the experimental value based upon centrifugal distortion constants and spacing of combination bands (≈300 cm⁻¹) and the theoretical value (320 cm⁻¹). Our experimental results suggest that the calculated harmonic frequencies for the two lowest bending motions which principally entail the in and out of plane displacement of the H₂ ligand (ν₆ and ν₉) may be overestimations.

Worthy of note is the increase in rotational constant for both Π-Π and Σ-Σ bands when the ν₁ stretch is excited. From an electrostatic point of view a shortening of the intermolecular bond is not unexpected as the quadrupole moment of H₂ is around 10% larger in the v=1 than the v=0 state (2.17×10⁻⁴⁰ Cm² for v=0, 2.40×10⁻⁴⁰ Cm² for v=1).⁴⁴ Thus exciting the ν₁ vibration might be expected to have the combined effects of shortening the intermolecular bond and deepening the intermolecular potential.

What of the barrier to the H₂ internal rotation? As mentioned in Sec. III the principal evidence for large amplitude

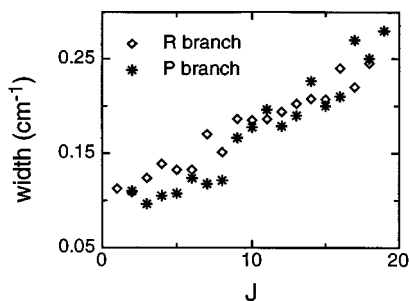


FIG. 10. Widths of P and R branch lines plotted as a function of J . The slopes of the two linear best fits are $0.008 \pm 0.002 \text{ cm}^{-1}$ (R branch) and $0.011 \pm 0.002 \text{ cm}^{-1}$ (P branch) somewhat larger than expected for the asymmetry doubling in a parallel transition of a prolate symmetric top (0.004 cm^{-1}).

hindered rotation might be expected to come from the magnitude of the asymmetry type doubling of lines in the $\Pi\leftarrow\Pi$ subband. In this regard we remark that although poor signal to noise ratio for the higher J lines makes it difficult to resolve doublets, we are able to estimate the combined width of the parity doublets in the P and R branch lines of the $\Pi\leftarrow\Pi$ subband. In Fig. 10, where rotational linewidths determined by averaging over several spectra are plotted as a function of J , it can be clearly seen that both P and R branch lines show a roughly linear J dependence. The linewidths increase rather more quickly than anticipated if the broadening was merely due to asymmetry doubling in a near prolate symmetric top where, using the geometrical parameters given by the *ab initio* calculations (Table I), one predicts a doubling that increases as $\Delta \approx 0.004 (J+1)$ for the R branch and $\Delta \approx 0.004 J$ for the P branch.⁴⁵ Best linear fits to the experimental data have slopes of $0.008 \pm 0.002 \text{ cm}^{-1}$ (R branch) and $0.011 \pm 0.002 \text{ cm}^{-1}$ (P branch), around twice the value expected for a prolate symmetric top, but more or less consistent with the value (0.007 cm^{-1}) expected from the hindered rotor analysis using the *ab initio* V_2 and V_4 terms presented in Sec. III.

Also in connection to the H_2 hindered rotation, we remark that in both vibrational states the $\Sigma\leftarrow\Sigma$ rotational constants are somewhat smaller than the $\Pi\leftarrow\Pi$ ones. Due to the large rotational constant of H_2 , even for substantial hindering potentials, the lowest Σ state contains a dominant proportion of $j=0$ basis functions ($c^2=0.77$ for the potential shown in Fig. 6). These functions are isotropic with respect to the intermolecular bond, and thus for the lower Σ level the H_2 samples angular regions where the intermolecular attraction is relatively weak ($\theta=0$) with a consequent bond destabilization (see Fig. 2). On the other hand, the lowest Π states are dominated by $j=1$ functions having a node in the weakly attractive linear configuration ($c^2=0.92$), being concentrated in the energetically more favorable T-shaped configuration ($\theta=\pi/2$) where attractive charge-quadrupole forces shorten the bond. Relative destabilization of Σ compared to Π manifolds has been previously noted in connection with the $\text{D}_2\text{-HF}$ complex which also possesses a T-shaped minimum, resulting from dipole-quadrupole interactions.²⁰

We now turn to a brief discussion of vibrational predissociation in the $\text{H}_2\text{-HCO}^+$ complex. Experience shows that vibrational predissociation in weakly bound complexes need not be a rapid process and that simple systems possessing energy far in excess of the dissociation threshold can be surprisingly long-lived. For example in time resolved studies we have inferred a vibrational predissociation lifetime of $220 \mu\text{s}$ for the $\text{N}_2^+\text{-He}$ complex possessing one quantum of the N-N stretching vibration.⁴⁶ In the present case there is evidence from broadening of rotational lines that depopulation of the upper level is extremely rapid, and that depending upon the actual vibrational level, occurs at rates of the order of $10^{10}\text{-}10^{12} \text{ s}^{-1}$. It is possible for homogeneous broadening to arise for two related reasons—intramolecular vibrational energy redistribution (IVR), where energy originally localized in the optically prepared level flows into a dense bath of nearly isoenergetic vibrational states, or direct vibrational predissociation with the prepared level directly coupled to the dissociative continuum.^{12,47} It is uncertain at this stage whether $\text{H}_2\text{-HCO}^+$ is really large enough to have a quasi-continuum of bound states at the energies of interest. In any case without undertaking time resolved predissociation studies it is difficult to distinguish between these two scenarios.

The $\text{H}_2\text{-HCO}^+$ predissociation/relaxation is decidedly nonstatistical, as the ν_1 state with over 1000 cm^{-1} more energy than the ν_2 state, has at least an order of magnitude slower vibrational predissociation rate. The variation is almost certainly due to differences in the coupling between the coordinate in which the energy is originally deposited and the other modes of the complex. The normal coordinate analysis reveals that the ν_1 vibration is almost a pure H_2 stretch motion entailing little motion of the H_2 ligand with respect to the HCO^+ . On the other hand, the ν_2 vibration involves appreciable relative movement of the subunits, presumably enhancing the opportunity for coupling with the dissociative coordinate ($\text{H}_2\cdots\text{HCO}^+$ stretch). Predissociation lifetimes for hydrogen bonded complexes have been noted to sensitively depend upon whether the bonded or nonbonded hydrogen is vibrationally excited, the former resulting in appreciably larger predissociation rates.⁴⁸

Our observations of slower IVR/vibrational predissociation rates for the H_2 stretch vibration compared to the other intramolecular motions agrees with findings for the $\text{H}_3\text{O}^+\text{-H}_2$ complex, in which the only vibrational transition to exhibit rotationally resolved structure is the ν_1 band, again involving excitation of the H-H stretching vibration. Okumura *et al.* have suggested that the strength of the intermolecular bond linking an H_2 ligand to a protonated molecule (e.g., H_3O^+ , HCO^+) can be correlated with the a reduction in the H-H stretching frequency from the free H_2 value.¹⁶ Such a connection comes about because the transfer of electron density from the $\text{H}_2\sigma$ bond to the protonated ion which establishes the incipient intermolecular chemical bond, also weakens the H_2 bond. It is possible that a similar connection exists between the intermolecular bond strength and the rate of vibrational predissociation after exciting the H-H stretch for various $\text{XH}^+\text{-H}_2$ complexes. As the intermolecular bond becomes stronger, the H-H stretching motion will be more effectively coupled to the remainder of the complex and thus to the dissociation coordinate, thereby en-

hancing the dissociation rate. There are theoretical⁴⁹ and experimental¹³ works that argue that the vibrational band shifts in complexes can be directly correlated to vibrational predissociation lifetimes, with the predissociation rate increasing with the square in the shift of the vibrational level.

The H₃O⁺-H₂ and H₂-HCO⁺ complexes have similar intermolecular bond strengths (3.1–3.9 kcal/mol for H₃O⁺-H₂¹⁶ and 3.9 kcal/mol for H₂-HCO⁺³) and H-H stretch vibrational frequencies (4046 cm⁻¹ for H₃O⁺-H₂ and 4060 cm⁻¹ for H₂-HCO⁺) and a comparison of dissociation rates would be interesting. Unfortunately, the existing H₃O⁺-H₂ spectrum in the H₂ stretch region appears to be laser linewidth limited (0.75 cm⁻¹) allowing only a lower estimate of 7 ps to be made for the ν₁ lifetime.¹⁶ In the case of the H₅⁺ complex, which has a binding energy of 7.1 kcal/mol with respect to dissociation into H₃⁺+H₂⁵⁰ and an H₂ stretch vibrational frequency of 3910 cm⁻¹, dissociation after exciting the ν₁ mode (at 3910 cm⁻¹) seems to occur on time scales of 1 ps or less, with no evidence for individual rotational lines in the spectrum, despite the rather large rotational constants expected for H₅⁺ (3.2 cm⁻¹).¹⁵

Above, we noted a *J* dependent increase in linewidths for the Π-Π subband, an effect proposed to be direct consequence of the large amplitude hindered rotation of the H₂. An alternative explanation might be that the broadening is homogeneous and arises from a vibrational predissociation rate that exhibits a linear *J* dependence, although this would seem to run counter to observations for neutral complexes where for a large number of species rotational linewidths are more or less independent of *J*.^{47,51} There are exceptions. For instance the hydrogen bonded C-H band of (HCN)₂ exhibits *J* dependent linewidths, the variations being supposed due to a *J* dependent coupling with a “dark” vibrational state more strongly connected to the dissociative continuum. However, in this case the linewidths do not increase linearly with *J*, but rather show the pattern expected for the *J* manifolds of two vibrational bands with slightly different rotational constants passing in and out of resonance.

So far we have not discussed the fate of the molecular photofragments arising from the vibrational predissociation. It is probable that energy in excess of that required to break the H₂⋯HCO⁺ bond will be partitioned between vibrational energy in HCO⁺ and H₂ rotational energy rather than into translation. This could possibly be tested by measuring fragment translational kinetic energies in a fast ion beam apparatus.

VI. CONCLUSIONS

In this paper we have sought to understand the interactions between H₂ and HCO⁺ in regions of intimate contact through experimental ir photodissociation and *ab initio* studies. From the experimental side we have been successful to the extent that the vibrational frequencies of two of the four intramolecular motions have been measured, the intermolecular stretch potential has been characterized both through centrifugal distortion parameters and through the observation of combination bands, and rotational constants for the end-over-end motion have been extracted. Measured properties and ones calculated at the QCISD(T) level of theory are in

good agreement and conclusively show that the complex has the T-shaped minimum energy geometry one expects from elementary electrostatic considerations. Several aspects of the story are unresolved particularly concerning the anisotropic parts of the interaction potential. In this regard it would be useful to carefully measure high *J* transitions in the *P* and *R* branches of the ν₁ band in order to determine whether they are homogeneously broadened or whether they are indeed split into asymmetry type doublets. Hopefully over time, further information on the intermolecular potential will come from other sources, including microwave measurements of collisional broadening of HCO⁺ rotational transitions by H₂, and indeed from microwave measurements of the complex itself.

ACKNOWLEDGMENT

This work is part of Project No. 20-36153.92 of *Schweizerischer Nationalfonds zur Förderung der wissenschaftlichen Forschung*.

- ¹E. Herbst and W. Klemperer, *Astrophys. J.* **185**, 505 (1973).
- ²F. C. Fehsenfeld, D. B. Dunkin, and E. E. Ferguson, *Astrophys. J.* **188**, 43 (1974).
- ³K. Hiraoka and P. Kebarle, *J. Chem. Phys.* **63**, 1688 (1975).
- ⁴R. H. Nobes and L. Radom, *Chem. Phys.* **60**, 1 (1981).
- ⁵D. A. Dixon, A. Komornicki, and W. P. Kraemer, *J. Chem. Phys.* **81**, 3603 (1984).
- ⁶D. Talbi and F. Pauzat, *Astron. Astrophys.* **229**, 253 (1990).
- ⁷D. Talbi and F. Pauzat, *Astron. Astrophys.* **181**, 394 (1987).
- ⁸S. A. Maluendes, A. D. McLean, and E. Herbst, *Astrophys. J.* **397**, 477 (1992).
- ⁹L. M. Ma, B. J. Smith, J. A. Pople, and L. Radom, *J. Am. Chem. Soc.* **113**, 7903 (1991).
- ¹⁰L. Radom, *Int. J. Mass Spectrom. Ion Proc.* **118/119**, 339 (1992).
- ¹¹T. Amano and H. E. Warner, *Astrophys. J.* **342**, L99 (1989).
- ¹²D. J. Nesbitt, *Chem. Rev.* **88**, 843 (1988).
- ¹³R. M. Miller, *Science* **240**, 447 (1988).
- ¹⁴R. C. Cohen and R. J. Saykally, *J. Phys. Chem.* **96**, 1024 (1992).
- ¹⁵M. Okumura, L. I. Yeh, J. D. Myers, and Y. T. Lee, *J. Chem. Phys.* **88**, 79 (1988).
- ¹⁶M. Okumura, L. I. Yeh, J. D. Myers, and Y. T. Lee, *J. Phys. Chem.* **94**, 3416 (1990).
- ¹⁷T. E. Gough, R. E. Miller, and G. Scoles, *Appl. Phys. Lett.* **30**, 338 (1977).
- ¹⁸A. R. W. McKellar and H. L. Welsh, *J. Chem. Phys.* **55**, 595 (1971).
- ¹⁹C. M. Lovejoy, D. D. Nelson, and D. J. Nesbitt, *J. Chem. Phys.* **87**, 5621 (1987).
- ²⁰C. M. Lovejoy, D. D. Nelson, and D. J. Nesbitt, *J. Chem. Phys.* **89**, 7180 (1988).
- ²¹E. J. Bieske, A. M. Soliva, and J. P. Maier, *J. Chem. Phys.* **94**, 4749 (1991).
- ²²E. J. Bieske, A. M. Soliva, A. Friedmann, and J. P. Maier, *J. Chem. Phys.* **100**, 4156 (1994).
- ²³E. J. Bieske, *Faraday Trans.* **91**, 1 (1995).
- ²⁴N. R. Daly, *Rev. Sci. Instrum.* **31**, 264 (1960).
- ²⁵M. J. McEwan, in *Advances in Gas Phase Ion Chemistry*, edited by N. G. Adams and L. M. Babcock (JAI, Greenwich, 1992).
- ²⁶E. J. Bieske, A. S. Soliva, M. Welker, and J. P. Maier, *J. Chem. Phys.* **93**, 4477 (1990).
- ²⁷A. J. Illies, M. F. Jarrold, and M. T. Bowers, *J. Chem. Phys.* **77**, 5847 (1982).
- ²⁸M. F. Jarrold, M. T. Bowers, D. J. DeFrees, A. D. McLean, and E. Herbst, *Astrophys. J.* **303**, 392 (1986).
- ²⁹C. J. F. Boettcher and P. Borderwijk, *Theory of Electric Polarization* (Elsevier, Amsterdam, 1978).
- ³⁰W. H. Flygare and R. C. Benson, *Mol. Phys.* **20**, 225 (1971).
- ³¹M. J. Frisch, G. W. Trucks, J. B. Foresman, M. A. Robb, M. Head-Gordon, E. S. Replogle, R. Gomperts, J. L. Andres, K. Raghavachari, J. S. Blinckley, C. Gonzalez, R. L. Martin, D. J. Fox, D. J. DeFrees, J. Baker, J. J. P.

- Stewart, and J. A. Pople, GAUSSIAN 92/DFT, Revision G.2 (Gaussian, Inc. Pittsburgh, 1993).
- ³²J. A. Pople, M. Head-Gordon, and J. Raghavachari, *J. Chem. Phys.* **87**, 5986 (1987).
- ³³R. Krishnan, J. S. Binkley, R. Seeger, and J. A. Pople, *J. Chem. Phys.* **72**, 650 (1980).
- ³⁴R. C. Woods, *Philos. Trans. R. Soc. London, Ser. A* **324**, 141 (1988).
- ³⁵K. P. Huber and G. Herzberg, *Molecular Spectra and Molecular Structure IV. Constants of Diatomic Molecules* (van Nostrand Reinhold, New York, 1979).
- ³⁶W. J. Hehre, L. Radom, P. v. R. Schleyer, and J. A. Pople, *Ab Initio Molecular Orbital Theory* (Wiley, New York, 1986).
- ³⁷R. J. Le Roy, University of Waterloo Chemical Physics Report CP-330 LEVEL 5.0 (1991).
- ³⁸J. M. Hutson, in *Advance in Molecular Dynamics and Collision Dynamics* (JAI, Greenwich, 1991).
- ³⁹D. C. Millen, *Can. J. Chem.* **63**, 1477 (1985).
- ⁴⁰R. G. Keese and A. W. Castleman, Jr., *J. Phys. Chem. Ref. Data* **15**, 1011 (1986).
- ⁴¹S. G. Lias, J. E. Bartmess, J. F. Liebman, J. L. Holmes, R. D. Levin, and W. G. Mallard, *J. Phys. Chem. Ref. Data* **17** (1988).
- ⁴²C. S. Gudeman, M. H. Begemann, J. Pfaff, and R. Saykally, *Phys. Rev. Lett.* **50**, 727 (1983).
- ⁴³A. R. W. McKellar, J. B. Burkholder, J. J. Orlando, and C. J. Howard, *J. Mol. Spectrosc.* **130**, 445 (1988).
- ⁴⁴L. M. Wolniewicz, *J. Chem. Phys.* **45**, 515 (1966).
- ⁴⁵C. H. Townes and A. L. Schawlow, *Microwave Spectroscopy* (Dover, New York, 1975).
- ⁴⁶E. J. Bieske, A. M. Soliva, A. Friedmann, and J. P. Maier, *J. Chem. Phys.* **96**, 4035 (1992).
- ⁴⁷R. E. Miller, *Acc. Chem. Res.* **23**, 10 (1990).
- ⁴⁸D. C. Dayton and R. E. Miller, *Chem. Phys. Lett.* **143**, 181 (1988).
- ⁴⁹R. J. LeRoy, M. R. Davies, and M. E. Lam, *J. Phys. Chem.* **95**, 2167 (1991).
- ⁵⁰K. Hiraoka, *J. Chem. Phys.* **87**, 4048 (1987).
- ⁵¹J. W. Bevan, in *Structure and Dynamics of Weakly Bound Molecular Complexes*, edited by A. Weber (Reidel, Dordrecht, 1987).